

Vapour-phase reduction and the synthesis of boron-based ceramic phases

Part II *The synthesis of hexagonal boron nitride phase*

SU JONG YOON*, A. JHA

Department of Materials Technology, Brunel University, Kingston Lane, UXBRIDGE UB8 3PH, Middlesex, UK

This investigation presents the results of the reduction–nitridation of boric anhydride (B_2O_3) in the nitrogen, nitrogen–hydrogen and nitrogen plus ammonia atmospheres for understanding the mechanism of boron nitride reaction. The effect of time on the reduction–nitridation reaction was studied at several preselected isotherms chosen between 1373 and 1773 K. The role of reaction parameters such as temperature, time and gas composition on the phase composition and microstructure is examined. In particular, the structural and stereochemical significance of BN-phase nucleation promoter in determining the crystallinity of h-BN phase is discussed. The importance of the sub-oxide BO gas in facilitating the formation of nanometre-size BN-phase is also explained. The relevance of the gas–solid phase equilibria in determining the stability of boron carbide phase is emphasized. The selected area electron diffraction analysis strongly hints to the evidence for a boron carbonitride phase ($B_4C_{1-x}N_x$). On the basis of our experimental findings, the significance of single-pellet study for h-BN powder manufacturing is also discussed in terms of the concepts for a reactor design.

1. Introduction

Hexagonal boron nitride is an important ceramic material and some of its major applications are briefly described in Part I [1] of this series. Beside their structural applications, the ceramic powder has more recently found use in TiB_2 -based ceramic–composite metal evaporator boats for the packaging industry. In this application, BN powder is invariably mixed as an electrically-resisting material with the electrically and thermally-conducting TiB_2 powder and thermally-conducting aluminium nitride. The electrical resistivity of hexagonal boron nitride depends upon the powder morphology and size. These two properties of hexagonal boron nitride (h-BN) powder determine the long-term thermal and electrical performance of the ceramic–composite evaporating metal containers.

Furthermore worldwide, there is a growing demand for fine BN powders for their use in the cosmetics industry. The quality of h-BN powder determines its use as a foundation material for make-up. H-BN powder has also a unique property for cosmetic application because it does not absorb moisture from the skin and leaves the surface in its natural condition. The traditional materials such as talcum powder adversely absorb surface moisture, thereby rendering the skin dry and damaged. The particle size, chemical characteristics of BN powders and their morphology are three important properties for cosmetics product

manufactures. These properties are determined by the processing conditions while B_2O_3 nitridation takes place in the presence of a reducing agent. A mechanism for controlling the powder morphology and structure is therefore an important part of the BN powder production technique.

In this part, we present the results from the synthesis of h-BN using the carbothermic reduction technique. In particular, the effect of processing variables on the particle size and the powder morphology is described. The experimental results presented below establish the relationship between the thermodynamic parameters and kinetic variables with the microstructure. Aspects of controlling the h-BN particle size is also examined in view of the nucleation process. As reported in Part I, the generation of either boric anhydride gas or BO gas and their nitridation in the presence of carbon takes place. The effect of the structure of carbon as a reducing agent on the crystallinity, of BN nuclei is also examined.

The present investigation also attempts to resolve a process-related issue arising from commercial BN powder manufacturing operations. A large majority of h-BN powder manufacturing principally adopts the carbothermic reduction of boric acid or boric anhydride and very often the operational temperatures are several hundred degrees celsius higher than the temperature predicted from the thermodynamic phase

* Present address: Department of Materials Science, Miryang University, Miryang 627-130, S. Korea.

equilibrium calculation. The undesirably high processing temperature raises the equipment running cost which in turn is added to the unit price of powder, thereby making the product less attractive for customers. Experimental results obtained in this investigation clearly shows that almost 100% conversion of boric acid to BN is possible in the temperature regime 1573 to 1773 K by using either nitrogen gas or nitrogen/hydrogen gas mixtures. Alternatively the injection of ammonia in the nitrogen gas stream will favour the conversion efficiency. The discussion of experimental results concludes with some proposed design features of an efficient BN reactor.

2. Experimental procedure

Granulated boron oxide (B_2O_3) of 99.999% purity was used as the starting material with carbon. The average granule size was 1–5 mm. The oxide granules were crushed in a steel mortar for 10 minutes and ground for more than 30 minutes in an agate mortar inside a dry glove box for the production of finer particles. The glove box powder handling and mixing reduces the risk of moisture contamination of boric oxide. Other types of boric anhydride (B_2O_3 pellet, diameter: 2.5 cm, 99.99% and > 98% purity) were also tested for the reduction experiments. The purity level of these powders were defined by the total boron present. Although a wide variety of virtually anhydrous boric oxides were used in the experiment, however no major variation in the weight loss as a result of either their purity or particle size was observed. The synthesis reaction was however found to be sensitive to moisture content which adversely contributed to the total weight loss. Activated charcoal of average size range 10–20 μm was also added as a reducing agent during the mixing process. Graphite powder of 99.99% purity and similar particle size range as activated charcoal was also used as a reductant.

For the sustenance of the nitridation reaction, $B_2O_3(l, s) + 3C(s) + N_2(g) = 2BN(s) + 3CO(g)$, more than the stoichiometric amount of carbon was added in the powder mixtures before compacting them into cylindrical pellets. Here s, l and g designate the solid, liquid and gaseous phases respectively. The pressure applied in the die was 20 MPa. However in order to understand the mechanism of the reduction reaction, less than the stoichiometric amount of carbon in the starting mixture was also added. This was necessary to analyse the volatilization loss of boric anhydride either as B_2O_3 gas or BO gas. A resistance-heated vertical furnace, shown in Fig. 1, was used for carrying out the high-temperature nitridation experiments. The schematic diagram shows the arrangement for the gas inlet and outlet.

The reduction–nitridation of B_2O_3/C mixtures were carried out at various preselected isotherms in the range 1373 to 1673 K. The selection of the isotherms was based on our thermodynamic calculations presented in Part I [1] of this series. The nitrogen flow was maintained at a rate of 500 ml min^{-1} whereas the flow rates for other gases used are specified in the table headings. Each pellet was left at an isotherm for

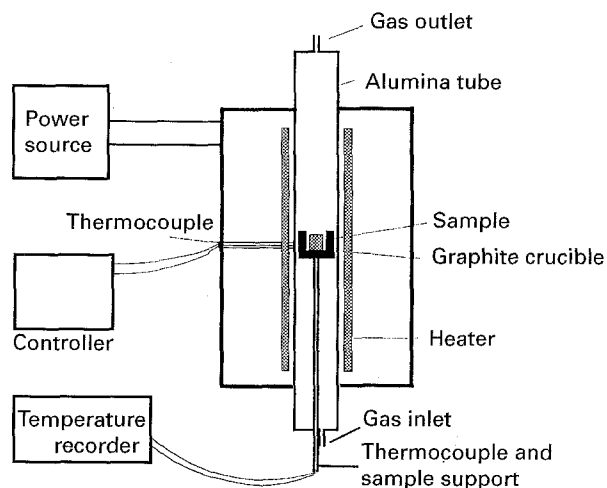


Figure 1 Schematic diagram of the resistance furnace with the arrangement of pelletized sample of boric anhydride and carbon inside the reaction tube.

a preselected period of time after which it was cooled down to room temperature and, the reaction product was analysed for the phases formed. For X-ray powder diffraction analysis (XRPD), the reacted pellets were carefully broken into two halves, one of which was ground in a mortar and pestle for a few minutes. The ground powder was then mounted on a sample holder for X-ray powder diffractometry using the CuK_{α} radiation (0.1541 nm). After powder diffraction, the results were stored on a personal computer and using a suitable software, the $CuK_{\alpha 2}$ peaks were subtracted after careful examination and comparison of the diffraction peaks with the JCPDS data files.

The second uncrushed half of the reduced and nitrided pellet was mounted for electron microscopic examination. A particular care was taken for handling the fragile pellets so that the as-reduced shape of the pellet could be retained for microscopic evaluation of the pore structure and the distribution of various phases formed.

3. Results

The results from the reduction–nitridation of boric oxide under different conditions are presented below. These results include the effects of the gas phase compositions, temperature, reaction time on the types of phases formed after reaction and their corresponding microstructures. The total reduction time was defined by the dwell time of the pellet in the isothermal zone.

3.1. The effects of time, the gas composition, type of carbon used and their proportions on the chemical and structural nature of phases produced

When the pressed pellets of the stoichiometric mixtures of boric oxide and carbon e.g. in the ratios of 1:2, 1:3 and 1:4 were nitrided in an atmosphere of nitrogen gas above 1473 K, h-BN formed. The formation of

TABLE I The effect of gas composition on the structure of BN phase formed. (Type of carbon used was activated charcoal. In ammonia/argon-hydrogen experiment, the flow rate NH_3 is 50 ml min^{-1} and Ar/H_2 100 ml min^{-1})

Starting materials	Temperature (K)	Time (h)	Gas composition	Produced phases
$\text{B}_2\text{O}_3 + 3\text{C}$	1573	4	N_2	h-BN
		1	$\text{N}_2 + \text{H}_2$ (15%) $\text{N}_2 + \text{H}_2$ (50%) $\text{NH}_3 + \text{Ar}/\text{H}_2$ (4%)	a-BN a-BN h-BN, Gra
	1473	8		a-BN, B_4C
	1523	4	N_2	a-BN, B_4C
	1573	5		a-BN, B_4C
	1673	8		a-BN, B_4C
$\text{B}_2\text{O}_3 + 4\text{C}$	1573	4	$\text{N}_2 + \text{H}_2$ (15%)	a-BN
	1573	4	$\text{N}_2 + \text{H}_2$ (50%)	a-BN
	1673	8	$\text{N}_2 + \text{H}_2$ (15%)	a-BN
	1573	0.5	$\text{NH}_3 + \text{Ar}/\text{H}_2$ (4%)	Gra, h-BN
X-ray diffraction figure reference			Breadth, B (0001-plane) (radian)	Approximate estimated grain size (nm)
Fig. 2(d)			$B_M = 7.68 \times 10^{-3}$	$< 75 \pm 5$
Fig. 2(c)			$B_M = 4.29 \times 10^{-2}$	$< 10 \pm 5$
Fig. 2(b)			$B_M = 4.60 \times 10^{-2}$	< 10 (amorphous)
Fig. 2(a)			$B_M = 3.87 \times 10^{-2}$	< 10 (amorphous)

The value of line broadening from a standard β -SiC powder of average size $1 \mu\text{m}$ is 0.01 degrees approximately $\theta_B = 35.77^\circ$, $t = 1 \mu\text{m}$.

TABLE II The effect of reaction temperature and time on the phases produced. Type of carbon used was activated charcoal. H_2 and N_2 compositions are indicated in the gas composition column of the table. Total flow rate of gas was 500 ml min^{-1}

Start materials	Temperature (K)	Time (h)	Gas composition	Produced phases
$\text{B}_2\text{O}_3 + 2\text{C}$	1373	2	N_2	B_2O_3 glass
	1473	2		B_2O_3 glass
	1573	2		B_2O_3 glass
	1573	4		h-BN
	1673	2		h-BN, B_4C
	1673	24		h-BN, (B_4C)
$\text{B}_2\text{O}_3 + 3\text{C}$	1573	4	N_2	h-BN
$\text{B}_2\text{O}_3 + 3\text{C}$	1473	4	$\text{N}_2 + \text{H}_2$ (50%)	a-BN
	1523	4		a-BN
	1573	4		a-BN
	1623	4		a-BN
	1673	4		a-BN
$\text{B}_2\text{O}_3 + 4\text{C}$	1473	8	N_2	a-BN, B_4C
	1523	8		a-BN, B_4C
	1573	4		a-BN, B_4C
	1573	8		a-BN, B_4C
	1673	4		a-BN, B_4C
	1673	8		a-BN, B_4C
	1773	8		a-BN, B_4C
$\text{B}_2\text{O}_3 + 4\text{C}$	1573	4	$\text{N}_2 + \text{H}_2$ (15%)	a-BN
	1573	4	$\text{N}_2 + \text{H}_2$ (35%)	a-BN
	1573	4	$\text{N}_2 + \text{H}_2$ (50%)	a-BN
	1673	8	$\text{N}_2 + \text{H}_2$ (15%)	a-BN

the crystalline form of h-BN was particularly favourable in the presence of graphite. However, when activated charcoal, having a semicrystalline structure, was used as a reducing agent, amorphous boron nitride (a-BN) was the predominant phase. It is likely that the degree of the crystallinity of a-BN phase be comparable with the activated charcoal which is found to be semicrystalline. The presence of boron

carbide was only confirmed in coexistence with a-BN. From the phase equilibrium calculations, the formation of boron carbide via carbothermic reduction occurs at 1862 K. Below this temperature, the carbide phase is unstable. In order to reduce the stability of B_4C phase with respect to BN in the presence of N_2 gas, it is important that the partial pressure of carbon monoxide in the reaction chamber must be

TABLE III The effect of reactivity and content of carbon on the phases produced. (Nitrogen flow rate 500 ml min⁻¹)

Carbon		Temperature (K)	Time (h)	Gas composition	Produced phases
Type	Content				
Active carbon	1C	1573	4	N ₂	h-BN
	2C	1573	4	N ₂	h-BN
	3C	1573	4	N ₂	h-BN
	4C	1523	8	N ₂	a-BN, B ₄ C
		1573	8		a-BN, B ₄ C
Graphite	2C	1673	8		a-BN, B ₄ C
		1773	8		a-BN, B ₄ C
	4C	1573	4	N ₂	Gra, B ₂ O ₃
		1523	8	N ₂	Gra, B ₂ O ₃
		1573	8		Gra, h-BN, B ₂ O ₃
	1673	8		Gra, B ₄ C, h-BN	
	1773	8		Gra, B ₄ C, h-BN	

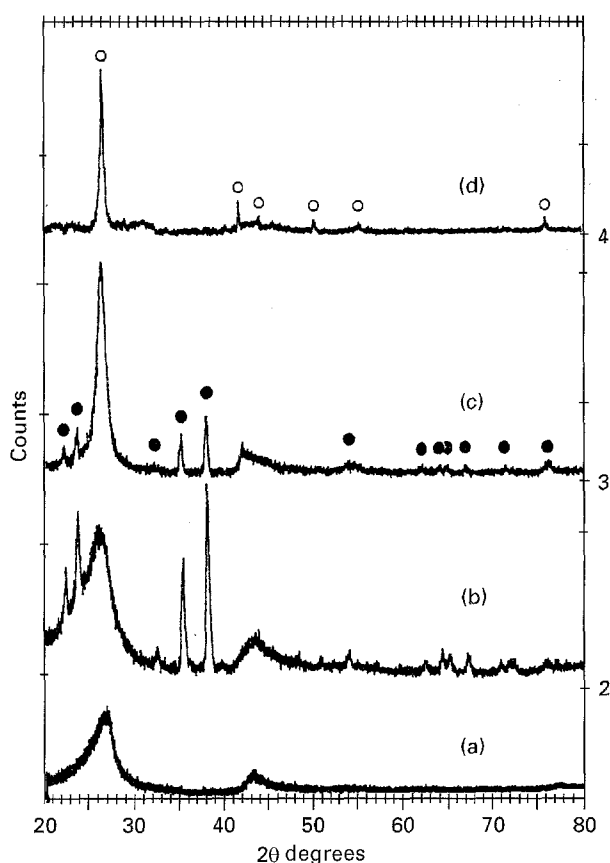


Figure 2 X-ray diffraction patterns of boron nitride (○) and boron carbide (●): (a) B₂O₃ + 3C, N₂ + H₂ (50%), 1673 K, 4 h; (b) B₂O₃ + 4C, N₂, 1773 K, 8 h; (c) B₂O₃ + 3C, N₂, 1673 K, 24 h; (d) B₂O₃ + 3C, N₂, 1573 K, 4 h. C, Activated charcoal.

lower than the equilibrium partial pressure for the stability of boron carbide i.e. $2B_2O_3(l, g) + 7C(s) = B_4C(s) + 6CO(g)$. The results under different experimental conditions are summarized in Tables I to III.

When the hydrogen gas was mixed with the reactive nitrogen in the presence of activated charcoal as a reducing agent, the crystallinity of BN phase changed. The a-BN phase was produced instead of h-BN. The formation of a-BN commenced with the concomitant disappearance of the carbide phase (see Table I). However the presence of ammonia gas as nitriding agent in the reaction chamber yielded a completely crystalline

h-BN structure irrespective of the type of carbon used for sustaining the reduction reaction. In view of the high-temperature decomposition of ammonia to nitrogen and hydrogen gas mixture ($2NH_3 = N_2 + 3H_2$), the formation of crystalline h-BN appears to be unusual because the presence of hydrogen in the nitrogen carrier gas, as shown above, does not yield h-BN. In the starting material, when activated charcoal was used as a reducing agent and the nitriding gas was ammonia, the residual carbon which originally had a semicrystalline structure, after the reduction-nitridation had also transformed into a graphitic structure.

The X-ray powder diffraction patterns of amorphous and crystalline h-BN are compared in Fig. 2. The full width of half maximum of the strongest h-BN peak was accurately measured by reading the intensity versus Bragg angle data file and by applying the following relationship

$$t = (0.9)\lambda/B \cos \theta_B, \quad (1)$$

the particle size is t , nm of the BN powders produced was estimated. Here θ_B is the Bragg angle in degrees, B is in radians and λ (CuK_α) is equal to 0.1541 nm. These results are summarized in Table I. The estimation of the particle size by using the line broadening technique has a minimum error of ± 5 nm and, hence the reported values are only an approximate comparison of the angular width, B , for different grain size of h-BN crystals formed under different conditions. The results in Table I also compares the corresponding B value for an average 1 μm size β-SiC powder. The range of the crystallinity achieved as a result of different types of reduction and nitridation conditions is unambiguously wide ranging from few to a hundred nanometres. The dimensions of h-BN microcrystals are evident from the photomicrographs shown in Figs 3, 4(a and b). The broader peaks in Fig. 2(a and b) almost appear amorphous. The sharp peaks of crystalline B₄C (1–5 μm in size (see Figs 3 and 4(b))) are superimposed on the X-ray powder diffraction pattern of amorphous BN.

When the carbon-to-oxide stoichiometric ratio in the pellet was less than 4, the nitridation in nitrogen atmosphere at 1673 K produced h-BN with B₄C phase within two hours of reduction. From

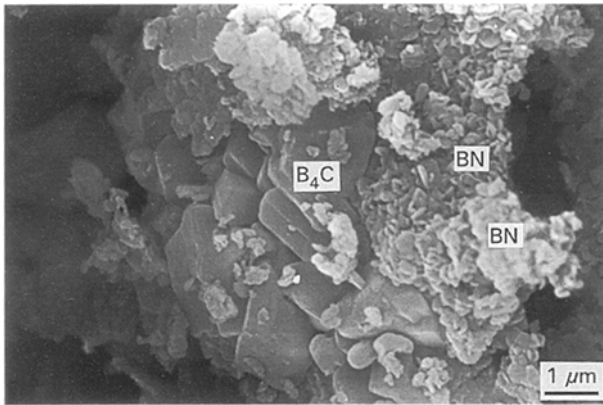


Figure 3 The SEM image of h-BN platelets produced from the transformation of B_4C crystals in the nitrogen atmosphere during the reduction-nitridation of $B_2O_3:C$ (activated charcoal) = 1:2 at 1673 K. N_2 flow rate was 750 ml min^{-1} .

Fig. 2(b and c), the relative intensities of boron carbide phase can be compared as a function of time and temperature. The trend for diminishing B_4C phase intensity was also confirmed at other isothermal conditions. By comparing the diffraction patterns in Fig. 2(b and c), it is evident that the relative intensities of B_4C phase is less with lower temperatures and longer times than in the case of high temperature reactions at

shorter times. Above the stoichiometric ratio of oxide-to-carbon equal to 1:3, there was no significant change in the relative intensities of powder diffraction pattern for the carbide and nitride phases formed. However when the excess carbon was present in the pellet, the carbide phase did not transform into h-BN phase in a nitrogen atmosphere even after prolonged period of time at 1773 K. The diminution of B_4C phase begins rapidly in the presence of hydrogen gas in the nitriding gas atmosphere. The experimental results also demonstrate that the diminution of B_4C phase begins at 15 vol% of hydrogen gas in the inlet nitrogen gas. This was an important observation which indicated that the stability of carbide and nitride phases depends upon the starting carbon content and also exclusively on the compositions of the nitriding gas atmosphere. The scanning electron micrograph of a partially reduced pellet, where the powder diffraction intensity of B_4C phase was reducing in favour of h-BN, is shown in Fig. 3. No significant change in the degree of the crystallinity of amorphous boron nitride phase with increasing time at a given temperature was observed.

The experimental results, summarized in Tables I to III, also point out to the relative stability of boron carbide in the presence of a nitriding atmosphere. As indicated earlier in Figs 4 and 5 in reference [1], the

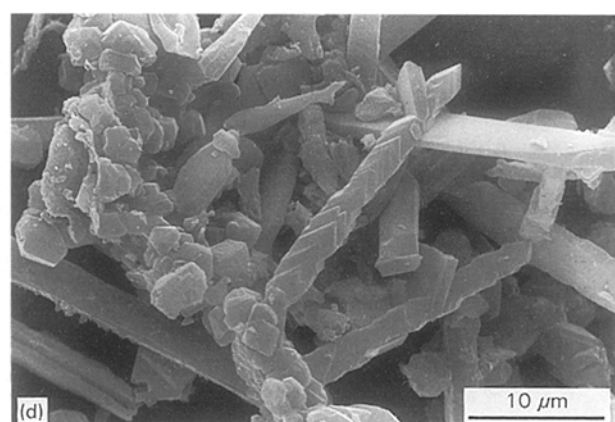
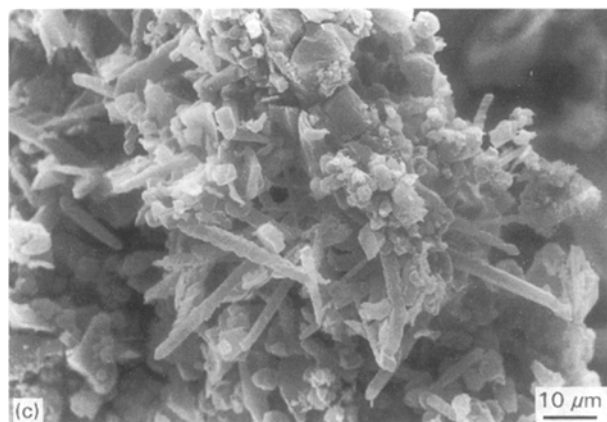
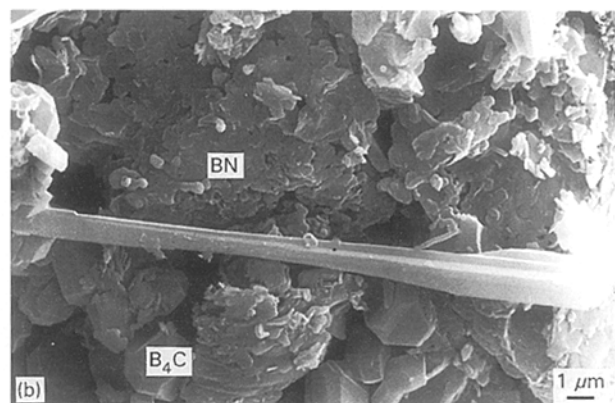
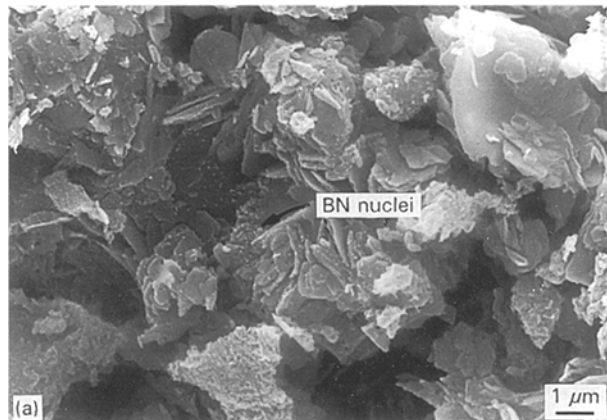


Figure 4 (a) The SEM image for the formation of sub-microscopic h-BN nuclei on the exposed surface. $B_2O_3:C$ (activated charcoal) = 1:3 at 1573 K in a N_2 stream (750 ml min^{-1}). (b) The SEM image of the stratified structure of h-BN coexisting with 1–5 μm B_4C crystals. A whisker of h-BN is also evident. $B_2O_3:C$ (graphite) = 1:4 at 1773 K in a N_2 stream (750 ml min^{-1}) after 8 h. (c) The growth of whiskers (SEM image) of h-BN phase from the boron carbide crystals buried underneath. $B_2O_3:C$ (activated charcoal) = 1:4 at 1773 K in a N_2 stream (750 ml min^{-1}) after 8 h. (d) The high magnification SEM micrograph of the whiskers in (c).

carbide phase is unstable at one atmosphere pressure of nitrogen gas over a wide range of temperature between 1300 and 1900 K. For this reason a few verification experiments were carried out at 1673 K by using partially-reduced and nitrided pellets where the presence of both carbide and nitride phases was confirmed by X-ray diffraction. As expected, these partially reduced pellets had unreacted activated charcoal. Pellet containing B_4C crystals were heat treated at 1673 K in an atmosphere of nitrogen and hydrogen gas where the composition of the gas mixture was 50 vol% N_2 and 50 vol% H_2 . The powder sample after heat treatment was analyzed by X-ray powder diffraction technique. By comparing the powder diffraction patterns before and after the annealing experiment, we observe a subtle change in the diffraction pattern. The powder pattern indicated that the carbide phase had become more crystalline which appears to be consistent with the observation of Thevenot [2] who reported that the crystallinity of boron carbide after annealing is known to increase. The improvement in the crystallinity may also be due to the loss of excess active carbon of semicrystalline nature as a gas phase (e.g. CH_4) from the pellet.

An additional reduction-nitridation experiment was also carried out. In this experiment, boric anhydride and active carbon mixture (1:3) was heated in a stream of nitrogen/hydrogen mixed gas for a short period of time (30 min). After this stage, the pellet was cooled down to room temperature from 1673 K. The X-ray powder diffraction pattern confirmed the presence of boron carbide phase which also formed with a-BN.

3.2. The effect of carbon content in the mixture along with the reduction temperature

The presence of graphitic carbon in the ratio of $C:B_2O_3 = 4:1$ at temperatures at and below 1523 K yielded graphitic carbon and boric anhydride glass. Above this temperature, the tendency for the formation of h-BN phase increased and eventually h-BN and boron carbide existed in equilibrium with the excess graphitic carbon (see Tables II and III). On the other hand, the presence of the activated charcoal in the ratio of 1:4 for boric oxide to carbon yielded a mixture of amorphous BN and B_4C in the nitrogen

atmosphere above 1473 K. When the stoichiometric proportion of carbon-to-oxide was lower than 4, the crystalline form of h-BN phase formed in the presence of active charcoal as reducing agent in a nitrogen atmosphere.

Only with lower stoichiometric proportions of carbon than 1:3, the reduction-nitridation of boric anhydride was incomplete. Due to this fixed ratio of carbon-to-oxide, the unreacted boric anhydride partially transformed into a glassy phase upon cooling and the remaining quantity volatilized as such at high temperatures while the pellet was being reduced. Above 1573 K, the tendency for the formation of either h-BN or a-BN was enhanced. This appears to be consistent with the reaction rate law i.e. the reduction rate increases with the increasing temperature. It was also confirmed that the reaction rate also increased with the reduction reaction surface area. Unfortunately in all the boron nitride experiments, it was difficult to accurately record the weight of the pellet after the reduction experiment had stopped. This was particularly due to poor pellet-forming tendency and friability of the powder mixtures containing activated charcoal. The hydrogen and NH_3 gases used also partially contributed to the total weight loss from the pellet due to an enhanced tendency for the formation of methane gas. This is the reason that none of the data tables in this paper include the values of percentage reduction.

From Tables I, II and III, we find that when activated charcoal was used as a reducing agent, the formation of BN started much closer to the predicted thermodynamic equilibrium temperature of 1316 K. At the end of the reaction, irrespective of the stoichiometric ratios of carbon-to-oxide shown in tables above, no free carbon was detected by X-ray powder diffraction pattern XRPD. The identification of graphitic carbon in the XRPD may have been obscured due to its structural similarity with the crystalline h-BN phase.

3.3. Microstructural evolution of boron nitride and boron carbide phases during the reduction-nitridation of B_2O_3

The experimental conditions for the photomicrographs discussed below are summarized in Table IV. In this table, the results from XRPD analysis are

TABLE IV Reduction-nitridation of boric oxide with activated charcoal (AC) and graphite (Gr). The nitriding gases were nitrogen and ammonia. N_2 flow rate: 500 ml min^{-1} at STP

Figures	Pellet mixture	Gas composition	Phases identified
4(a)	$B_2O_3 + 3C(AC)$ 1573 K, 4 h	N_2	h-BN
4(b)	$B_2O_3 + 4C(Gr)$ 1773 K, 8 h	N_2	Gra, h-BN, B_4C
4(c)	$B_2O_3 + 4C(AC)$ 1773 K, 8 h	N_2	a-BN, B_4C
4(d)	$B_2O_3 + 2C(AC)$ 1773 K, 2 h	$NH_3 = 50 \text{ ml min}^{-1}$ $Ar + 4\% H_2 = 100 \text{ ml/min}^{-1}$	h-BN, B_4C (B_4C was present in small proportions)

also included. From this the phases produced after reduction were identified.

The microstructure of the reaction product formed in the nitrogen atmosphere, for example, are shown in Fig. 4(a–d). In Fig. 4(a), we see the evidence for the nucleation of h-BN crystals. The “dotted phase” seen as white spots in the micrograph are the nuclei of h-BN which have formed on already growing h-BN crystals. In the microstructure shown below, the smaller nuclei grow into a mass of dense platelets (light grey areas). Evidently the photomicrographs strongly point to a process of the nucleation of h-BN crystalline phase and its simultaneous growth under a given experimental condition. In this particular case, the amount of activated charcoal used was barely sufficient to convert B_2O_3 completely to BN (oxide:carbon = 1:3), and towards the end of the reduction reaction a few nuclei of h-BN must have formed. However these submicroscopic h-BN nuclei were unable to sustain their growth. It may be due to this reason that they stand out in the micrograph as a unique evidence for the continuation of nucleation process. By comparing the micrometre bar with the size of the nucleated phase, it appears that the nuclei are 10 to 30 nm in size. Whereas the growing crystals have diameters from over 200 to 2000 nm but their thickness is only limited to an average of 10 to 20 nm. Microstructural evidence strongly supports the line broadening measurements and confirms that the c-axis of h-BN is not the predominant growth direction during the synthesis of h-BN.

The crystal growth also appears to have contributed to larger clusters of average 10 μm in size. This is evident in all micrographs of BN produced in a nitrogen atmosphere. The microstructure in Fig. 4(b) reveals the presence of a uniform size of B_4C crystals (dark grey) and the stratified h-BN structure (also dark grey) along with carbon which appears dark in this micrograph. The growth of whiskers frequently found as a predominant feature of the overall microstructure is also quite apparent from the photomicrographs shown in Fig. 4c. The whiskers of BN and rhombohedral crystals are growing from the mass of B_4C crystals. This high magnification micrograph undoubtedly shows two types of crystal growth morphologies: namely the “blade shape” and “rhombohedral-faceted” whiskers. These two morphologies were found to be equally abundant in the reaction product. The formation of these whiskers in this case may have been a major contributory factor in enhancing the overall crystallinity of the powder diffraction pattern as indicated in Section 3.1.

Fig. 5(a and b) show the microstructures of BN crystals produced in the ammonia atmosphere. These two micrographs are in sharp contrast with the microstructure produced from N_2 gas atmosphere shown in Fig. 4(a–d). The nucleation of crystals appears to be occurring uniformly along the surface of “hollow” columns. The hole along the growth axis of the tubular structure is evident in this figure. There are much larger number of nuclei per unit area of h-BN in ammonia atmosphere than found with the nitrogen gas. This difference in the number of nuclei per

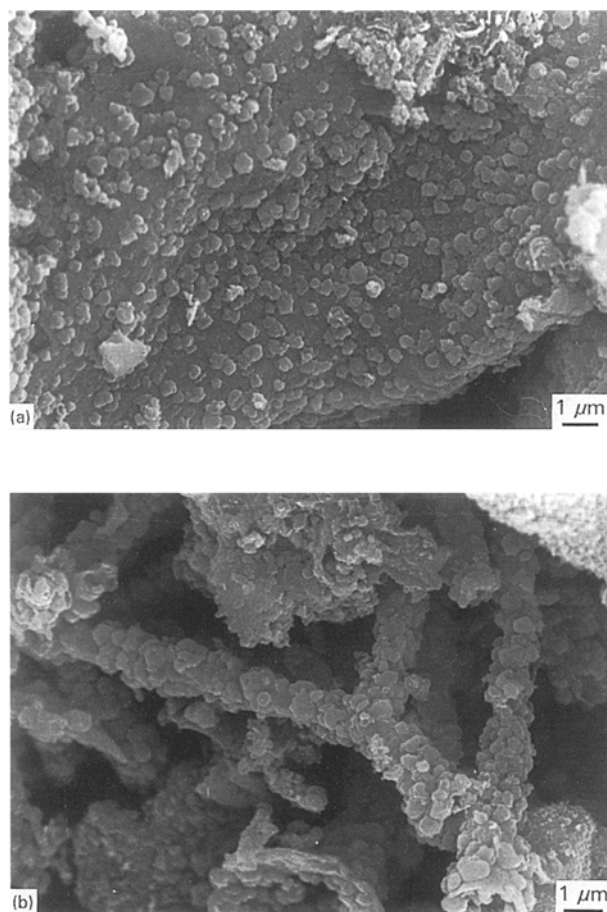
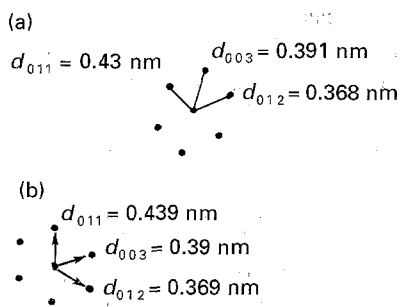
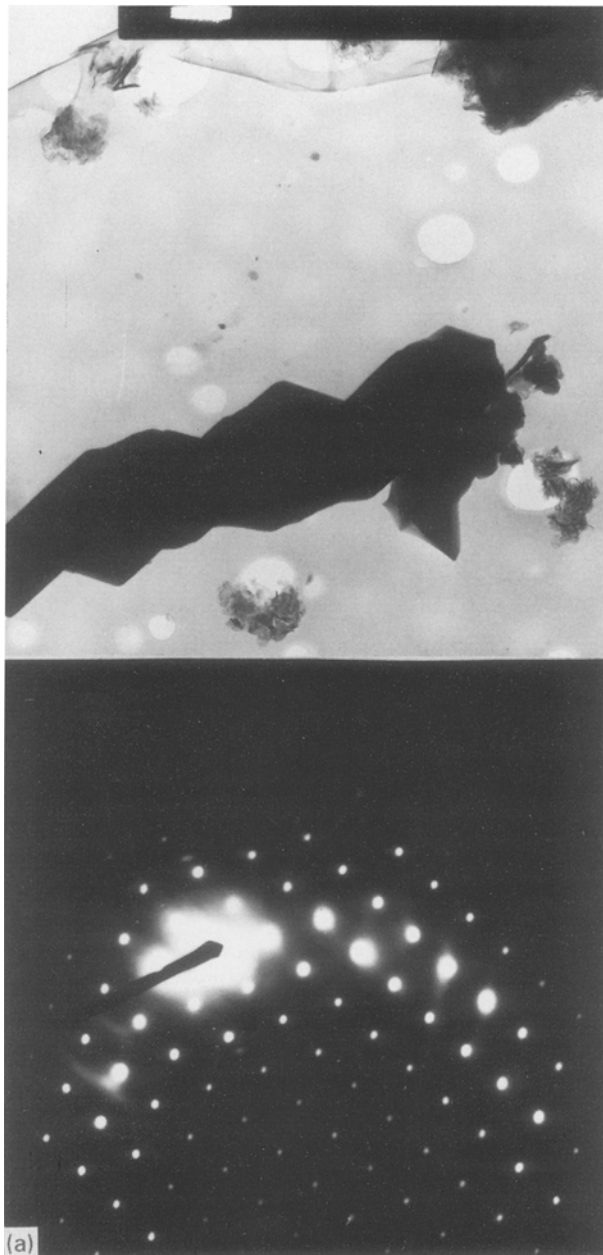


Figure 5 (a) The SEM image of the structure of h-BN whisker surface with large number of surface nuclei produced in the presence of cracked ammonia, and Ar-4% H_2 gas mixture. Ammonia gas flow: 50 ml min^{-1} , Ar + 4% $H_2 = 100 \text{ ml min}^{-1}$. $B_2O_3:C$ (activated charcoal) = 1:2 at 1773 K after 2 h. (b) The tube-like growth of h-BN under the condition described in (a).

unit area can be verified by the comparison of the two types of micrographs. Also the nuclei in NH_3 atmosphere appear to have grown at a faster rate at 1773 K than the same phase formed in the nitrogen gas atmosphere under identical temperature condition. The dense crystalline mass produced underneath the growing nuclei are over 50 μm .

The formation of hollow h-BN whiskers is consistent with the morphology of tubular carbon reported in the literature [3], which was also observed in this investigation while reducing $B_2O_3 + 2C$ mixture in a graphite crucible. The transmission electron micrograph of the tubular carbon is shown in reference [3] which has an unusual bamboo-like structure with a hole along the growth axis. The bamboo-like knots in the h-BN microstructure, produced in the ammonia/ $Ar-H_2$ atmosphere is completely absent.

The transmission electron micrograph analysis also revealed some crystal structure information for the whiskers with rhombohedral cross-section. The bright field micrographs and the corresponding selected area diffraction patterns SADP are shown in Fig. 6(a and b). The SADPs of the micrographs confirm the presence of crystallographic faults and stress accumulated in the crystals. These defect structures in the bright-field TEM image of the rhombohedral crystals, which is also the Bravais lattice of B_4C crystals, can also be



ascertained from the streaking of the diffraction spots. A similar type of features in the diffraction pattern of β -SiC whiskers was also reported earlier [4]. It is commonly known that the whisker growth is aided by the motion of screw dislocations as a result of which the associated stress due to dislocation motions accumulate along the growth direction. The magnitude of the accumulated stress depends upon the dimensions of whiskers as has been shown by Eshelby [5]. The d -spacings of these two types of crystals are shown on

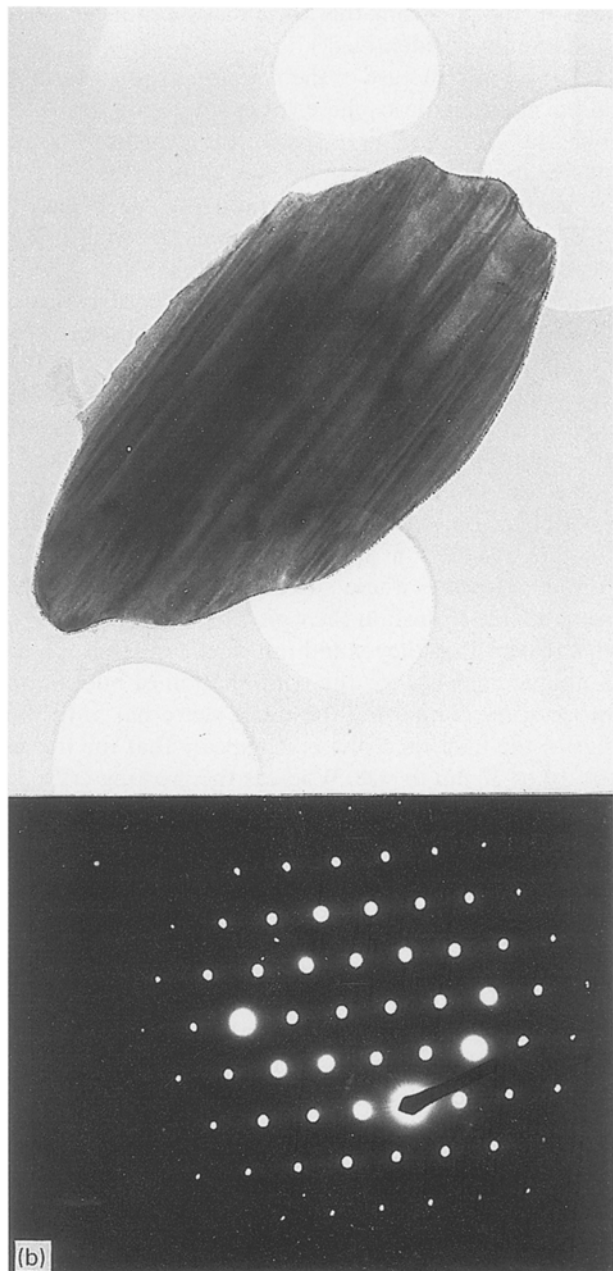


Figure 6 (a) Transmission electron micrographs of nitrided B_4C crystals with accompanying selected area diffraction pattern. Magnification $\times 30000$. (b) Transmission electron micrographs of nitrided B_4C crystals with accompanying selected area diffraction pattern. Magnification $\times 3000$. Experimental conditions: $B_2O_3:C$ (charcoal + graphite) = 1:3, 1673 K, 24 h

the corresponding schematic diagrams and the measured values do not agree with the reported d -values of either pure boron carbide or pure boron nitride. The best approximate is a smaller B_4C lattice with $d(0\bar{1}1) = 0.439 \text{ nm}$, $d(003) = 0.390 \text{ nm}$ and $d(012) = 0.369 \text{ nm}$ (see SADP accompanying Fig. 6(a)). The pure crystalline B_4C lattice has $d(0\bar{1}1) = 0.4499 \text{ nm}$, $d(003) = 0.4033 \text{ nm}$ and $d(012) = 0.3783 \text{ nm}$. In the second diffraction pattern in Fig. 6(b), the d -values are: $d(0\bar{1}1) = 0.434 \text{ nm}$, $d(003) = 0.391 \text{ nm}$ and $d(012) = 0.368 \text{ nm}$. The d -spacing data based on boron carbide approximant indicates that the composition of the crystals may be slightly different from either c-saturated or B-rich B_4C . On the basis of the

TABLE V The calculated lattice parameters and d -spacings (From equation 2) of unknown nitrided B_4C crystals

Name	d -spacing (nm)			Lattice parameters (nm)
	011	003	012	
B_4C C-saturated Fig. III-6	0.4499	0.4033	0.3783	$a = 0.5607$ $c = 1.2095$
Fig. III-7	0.438	0.390	0.369	$a = 0.550$ $c = 1.170$
	0.439	0.391	0.368	$a = 0.546$ $c = 1.174$
	hk1	d (nm)		
	(101)	0.4146		
	(003)	0.3900		
	(012)	0.3690		
	(110)	0.2750		
	(104)	0.2492		
	(021)	0.2332		
	(113)	0.2242		
	(024)	0.1847		
	(211)	0.1779		
	(205)	0.1669		
	(107)	0.1577		
	(214)	0.1533		
	(303)	0.1470		
	(125)	0.1427		
	(018)	0.1398		
	(220)	0.1375		
	(131)	0.1312		
	(223)	0.1297		

comparison of the d -spacings of the approximant with that of the pure carbide phase reported by Thevenot [2], we find that on an average there appears to be a reduction of 2.5 to 3.0% in the cell dimension of the pure carbide lattice. This may either be due to the presence of vacant c-sites in the B_4C structure or due to the partial replacement of carbon atoms by nitrogen atoms in the structure. The B-rich B_4C has larger lattice parameters than B_4C crystalline phase in equilibrium with carbon. Boron carbide formed in this investigation is expected to be a c-saturated B_4C . In the presence of nitrogen-hydrogen gas mixture and ammonia, the carbonitride reaction: $B_4C + (x/2)N_2 + 2xH_2 = B_4C_{1-x}N_x + xCH_4$ (g) is likely to take place. The nitrogen atoms, having a very similar atomic radius as carbon, are expected to be in a similar type of co-ordination shell as their carbon analogues in the crystal structure of carbon-saturated B_4C . Using Equation 2 for the hexagonal crystal lattice, the lattice parameters of the unknown crystals were determined and these are summarized in Table V below.

$$\frac{1}{d^2} = \frac{4}{3} \left(\frac{h^2 + hk + k^2}{a^2} \right) + \frac{l^2}{c^2} \quad (2)$$

The measured d -spacing for the Bragg reflection (003) for these micrographs were used for calculating the c -axis of the hexagonal lattice using the above equation, whereas 011 and 012 reflections along with the dimension of c -axis yielded the value of " a " dimension of the hexagonal lattice. The 011 reflection is a low angle reflection and has a correspondingly larger error. For obtaining a better accuracy of the " a " lattice parameter, the Miller indices from the reflections of 012

planes was substituted in Equation 2. The volume fraction of crystals discussed above in the reaction product appeared to be fairly small for the detection limit of the XRPD technique. Due to this reason, other complementary interplanar distances were not accurately obtained from the XRPD pattern. On the basis of the d -spacing data and the knowledge of the diffraction vectors, using JCPDS powder diffraction file for B_4C crystals, the remaining d -spacings were computed by using Equation 2. These results are compiled in Table V for comparative purposes.

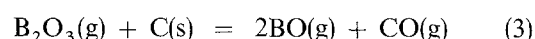
4. Discussion

The reduction of boric anhydride (B_2O_3) under different conditions discussed above yielded boron carbide and the two main structural forms of hexagonal boron nitride. On the basis of these results, the mechanism of the formation of crystalline and semicrystalline (amorphous) BN and the stability of B_4C under nitriding conditions are discussed.

4.1. The mechanism of B_2O_3 volatilization and reduction in the vapour state

Boron oxide (B_2O_3) has a tendency to volatilize above its melting point at 723 K, and the equation for the temperature dependence of its vapour pressure is reported elsewhere [1] from which the values of the enthalpy and entropy of evaporation can be derived for the volatilization reaction: $B_2O_3(l) = B_2O_3(g)$. The equation for the free energy of vaporization of B_2O_3 liquid to B_2O_3 gas is $360.053 - 0.1867T$ kJ mol⁻¹ K⁻¹ [1]. The vapour pressure of B_2O_3 in the reaction chamber used for BN synthesis is expected to be of the order of 10.13 Pa at 1423 K and rises exponentially with the increasing temperature.

As indicated earlier [1] another likely species of boron oxide gas is commonly known as "BO" gas and has been reported to be stable only under either a reducing or an inert gas condition. "BO" gas can therefore form from B_2O_3 gas at elevated temperatures via



for which the standard Gibbs free energy change is equal to $746.79 - 0.287T$ kJ mol⁻¹. The relevant free energy data have been obtained from references [1] and [6]. The temperature dependence of BO gas partial pressure at $P_{CO} = 101.3$ Pa (10^{-3} atm) is compared with the partial pressure of B_2O_3 gas in Fig. 7. As expected, the partial pressure of BO gas is smaller than B_2O_3 gas at any temperature between 500 and 2500 K. Experimental results from the reduction-nitridation suggest that the presence of both gaseous species in the reaction chamber is critical for the formation of BN and B_4C crystals. Under the reducing atmosphere in the reaction chamber, continuously flushed with a stream of N_2 purge gas, the partial pressure of BO gas at a given temperature is determined by the presence of the residual CO gas in the atmosphere and the partial pressure of boric oxide gas. At a constant temperature, as the value of CO partial pressure decreases, the pressure of BO gas in

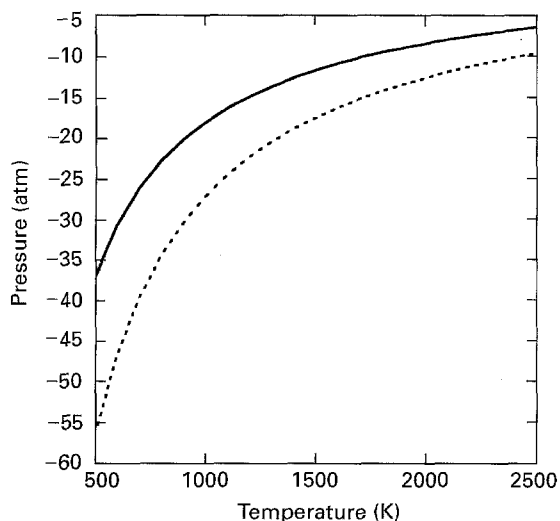


Figure 7 A comparison of the computed partial pressures of boric oxide (—) and boron monoxide (---) gases over a temperature range of 500 K and 2000 K.

the reaction chamber will increase in accordance with the equilibrium relationship

$$K = \frac{(p_{\text{BO}})^2 p_{\text{CO}}}{p_{\text{B}_2\text{O}_3} a_{\text{C}}} \quad (4)$$

for arbitrarily fixed activities of carbon and B_2O_3 gases. It is therefore expected that each reduction-nitridation experiment corresponds to a unique BO, CO and B_2O_3 partial pressures because of a variation in the reduction reaction parameters such as the carbon content and the temperature.

4.2. Formation of BN and B_4C during reduction-nitridation of boric anhydride at high temperatures in N_2 atmosphere

In the presence of a reducing agent, the gaseous form of B_2O_3 reduces to its lower diatomic gaseous form as discussed above. The formation of BO gas provides a large surface area for the reduction reaction via which either BN or B_4C begins to nucleate and grow. From the phase equilibria in the B-C-N-O system, discussed previously [1], the regions of phase stability of BN and B_4C are defined over a range of temperature and partial pressures of N_2 and BO gases.

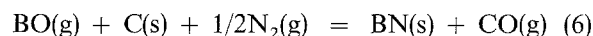
From the XRPD results, the following mechanism for the formation of h-BN phase is proposed. The formation of BO gas via Equation 3 is strongly dependent upon the partial pressure of CO gas in the surrounding pores of the pellet containing boric anhydride and carbon. For example, at 1673 K the equilibrium partial pressure of BO gas at an arbitrarily chosen value of P_{CO} equal to 101.3 Pa (10^{-3} atm) is of the order of 222.8 Pa (2.2×10^{-3} atm) which is twice as large as CO partial pressure. As pointed out in Equation 2, the lower CO pressure will raise the equilibrium partial pressure of BO gas in the surrounding atmosphere. Thermodynamic calculations also indicate that at $P_{\text{CO}} = 101.3$ Pa (10^{-3} atm), the equilibrium partial pressure of CO_2 from the Boudouard

reaction is of the order of 303.9 Pa (3×10^{-3} atm) at 1673 K assuming that the activity of carbon is unity.

In a continuously flushed reaction chamber such as one used above, the partial pressure of CO gas will never be allowed to reach the equilibrium value and therefore the value of P_{BO} is expected to be larger than P_{CO} . This condition is favourable for the formation of both BN and B_4C crystals, however, more so for the latter due to the conditions imposed by the stoichiometry. With the increasing temperature, the value of P_{BO} will rise at a given CO pressure. The presence of BO gas in the pores of pellet in contact with solid carbon and the lack of sufficient N_2 gas creates a favourable condition for the formation of B_4C phase via

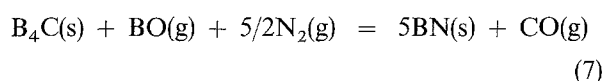


instead of the thermodynamically favourable BN phase. The preference of B_4C over BN phase in nitrogen atmosphere indicates that if we assume



for which the value of ΔG° equals to $-361380 + 90.7T$ J mol $^{-1}$, the value of $(P_{\text{N}_2})^{1/2} = (a_{\text{N}})$ is of the order of 10^{-10} . This value indicates that the core of the pellet during experiment appears to be completely starved of nitrogen gas, thereby rendering the formation of h-BN crystals thermodynamically impossible. Due to this nitrogen deficiency away from the circumferential region into the centre of the pellet, the formation of boron carbide is greatly enhanced. The above chemical reaction hypothesis was supported experimentally by verifying the presence of B_4C phase in the XRPD pattern of the powder samples from the core regions of the pellet.

The formation of B_4C reaction overwhelms the reduction-nitridation process in the initial stage of the overall nitridation process. This has also been confirmed experimentally by performing a short-time reduction-nitridation experiment discussed in Subsection 3.1. Experimental results also pointed out that when the proportion of carbon to B_2O_3 is less than 3:1, the relative intensity of the powder diffraction peak for the B_4C phase diminished with prolonged reduction time. This result indicated that soon after the early stage of the reduction-nitridation reaction, B_4C gradually transformed to BN. The relative diffraction intensity of the nitride phase increased at the expense of B_4C . On the basis of the microscopic and powder diffraction evidences, we propose that the initial period of reduction leading to Equation 5 is followed by the conversion of B_4C to BN in the presence of the BO gas in the surrounding pore volume space via

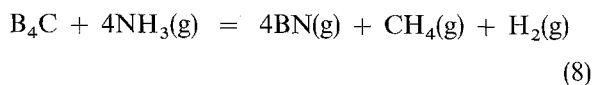


reaction. The value of Gibbs free energy change is ΔG° equals $-1322822 + 435.5T$ J mol $^{-1}$ of B_4C . The formation of BN via Equation 6 in the absence of B_4C competes with the conversion of BO gas to BN via Equation 7 in the presence of B_4C .

The relative dominance of thermodynamic equilibrium for Equations 5, 6 and 7 can be quantified by calculating the value of the equilibrium partial pressures of BO gas at a given temperature. For example at 1673 K and at a given partial pressure of CO (say 101.3 Pa). The computed equilibrium partial pressures are 2.53×10^{-2} Pa (2.5×10^{-7} atm), 2.83×10^{-5} Pa (2.8×10^{-10} atm) and 2.83×10^{-17} Pa (2.8×10^{-22} atm), respectively. The minimum computed partial pressure of BO for Equation 7 makes this reaction more favourable than the other two. The relative difference in the free energy (ΔG_v) can be quantified by taking the natural logarithm of the ratio of BO partial pressures multiplied by the absolute temperature and the universal gas constant i.e. $\Delta G_v = -RT \ln(P_{BO}^{eq5}/P_{BO}^{eq7})$. This is the Gibbs volume free energy for determining the nucleation rate and is inversely related with the square of ΔG_v i.e. $\Delta G^* \propto 1/(\Delta G_v)^2$. The values of ΔG_v derived for 5 and 6, and 5 and 7 are -96 kJ and -480 kJ respectively which means that if the surface energy contribution for the carbide-to-nitride conversion is kept identical, then the estimated nucleation rate for BN formation via Equations 5 and 7 is several thousand times faster than the synthesis route 5 and 6. In Fig. 3, where the nitrogen and BO gas mixture appeared to have come in physical contact with the exposed chunky boron carbide crystals, there is a strong evidence for copious nucleation of platelet-like h-BN phase. The pattern of nucleation of h-BN on B_4C crystal is in sharp contrast with boron nitride phase having a layered structure in Fig. 4(b). On the exposed surface of the stratified BN structure, there are some nuclei growing along the surface.

4.3. Reduction-nitridation of B_2O_3 in the presence of carbon in ammonia atmosphere

The nitridation of B_2O_3 with NH_3 in the presence of carbon differs in two ways. First of all the partial pressure of nitrogen produced from the decomposition of ammonia gas is higher than the partial pressure of pure N_2 used at atmospheric pressure. This is due to the relatively favourable thermodynamic conditions. The higher N_2 pressure favours the decomposition of B_4C phase via



reaction. The standard Gibbs free energy change is $\Delta G^\circ = -837135 - 10.54T \text{ J mol}^{-1}$. The second important role of ammonia gas is that it also favours the formation of BN via $BO(g) + NH_3(g) + C(s) = BN(s) + 3/2H_2(g) + CO(g)$. The standard Gibbs free energy difference for the two BO gas reduction-nitridation reactions: $BO(g) + NH_3(g) + C(s) = BN(s) + 3/2H_2(g) + CO(g)$ and $BO(g) + N_2(g) + C(s) = BN(s) + CO(g)$ is summarized in Table VI. As a result of this difference in the nitriding chemical potential, the condition for the nucleation of BN also changes in favour of the ammonia gas. The differential in the thermodynamic driving force related with the

TABLE VI A comparison of the Gibbs free energy of formation (ΔG°) of h-BN phase as a function of temperature via nitridation and reduction of BO gas in the presence of carbon with nitrogen and ammonia gas

T (K)	ΔG° (J) for $BO(g) + \frac{1}{2}N_2(g)$ $= BN + CO(g)$	ΔG° (J) for $BO(g) + C + NH_3(g)$ $= BN + \frac{1}{2}H_2(g) + CO(g)$
750	-293 395	-327 055
1000	-270 720	-333 535
1250	-248 045	-340 000
1500	-225 370	-346 480
1750	-202 695	-352 955
2000	-180 020	-359 430

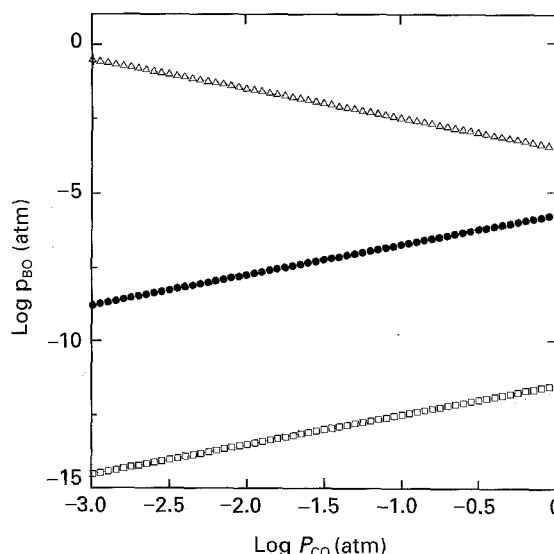
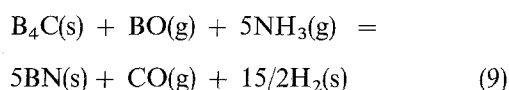


Figure 8 A plot of $\log P_{BO}$ (atm) against $\log P_{CO}$ (atm) at 1773 K for the following reactions. $BO(g) + C(s) + NH_3(g) = BN(s) + 1/2H_2(g) + CO(g)$ (\square); $BO(g) + C(s) + 1/2N_2(g) = BN(s) + CO(g)$ (\bullet); $B_2O_3(g) + C(s) = 2 BO(g) + CO(g)$ (Δ).

barrier for nucleation of BN phase (ΔG^*) can be determined graphically by plotting $\log P_{BO} - \log P_{CO}$ diagram at a given temperature and partial pressures of gases mentioned above. The relationship between $\log P_{BO}$ and $\log P_{CO}$ for ammonia nitridation of boric anhydride is compared with the nitridation condition with pure N_2 gas in Fig. 8. From this figure, it is evident that under a given set of conditions, the equilibrium partial pressure of BO for ammonia is significantly lower than the partial pressure of BO for N_2 gas. The presence of a large number of growing nuclei of h-BN phase, shown in Fig. 5(a and b), which is strongly dependent on the Gibbs volume free energy change (ΔG_v) supports the above thermodynamic calculations. The observed nucleation frequency with ammonia nitridation appears to be similar to that observed in the case of the transformation of B_4C crystals in Fig. 3.

During the nitriding reaction with ammonia, an Ar-4% H_2 gas mixture was used. The reaction equilibrium suggests that at a constant temperature and fixed CO and NH_3 partial pressures, the partial pressure of hydrogen will determine the activity of BN which means that the lower the value of P_{H_2} , the higher will be thermodynamic activity of BN phase, leading to

a higher rate of nucleation. In a similar way thermodynamically it can be proven that



is more favourable than Equations 6 and 7.

Besides the contribution of ammonia gas in assisting the nucleation process, the large differential in the Gibbs free energy between the BO generation and consumption reactions also favours an accelerated epitaxial growth of h-BN, as can be seen in Fig. 5.

4.4. Conditions for the formation of a-BN and h-BN

The possibility of obtaining a wide range of structural variety of hexagonal BN phase is one of the most important features of the present investigation. Results shown in Tables I and III indicated that the crystallinity of h-BN was dependent on three factors: (a) the structural chemistry and the physical state of the substrate, (b) gas composition and (c) temperature. Their roles in determining the structure of h-BN is explained below.

The formation of the amorphous form of h-BN takes place in the presence of activated charcoal in the starting mixture. The proportion of charcoal in the mixture must be equal to the minimum stoichiometric requirement for a complete conversion of boric anhydride to BN i.e. $\text{B}_2\text{O}_3:\text{C}$ must be equal to at least 1:3. In the presence of excess activated charcoal, which has a semicrystalline graphite-like network structure, boron nitride phase nucleates epitaxially on the surface of the active carbon. The constituent atoms in the nuclei assume the local structure order and then continue to grow as an amorphous phase. However, when the ratio of active carbon-to-oxide drops to 3:1 and lower, in the gas phase, the concentration of B_2O_3 species is expected to rise due to the reduced surface area for BO formation reaction. Due to this, the BO concentration is expected to be lower than when $\text{C}:\text{B}_2\text{O}_3$ is 3:1. At higher concentrations of B_2O_3 gas, which has an sp^2 hybridized molecular structure, the formation of h-BN phase is promoted via an sp^2 -hybridized gas-phase nucleation precursor. This is the reason that the sp^2 -hybridized h-BN structure forms when $\text{C}:\text{B}_2\text{O}_3 = 3:1$. This observation also appears to be consistent with the reduction-nitridation of boric oxide in the presence of graphite and ammonia, both being the sp^2 -hybridized structures. The line broadening data and the thickness of the microcrystallites, shown in micrographs above, are consistent with the stereochemical mechanism of h-BN crystal nucleation. The growth of crystals is faster along the *a*-axis than along the *c*-axis because of the presence of sp^2 -hybridized gas and solid phase precursors for facilitating the nucleation of h-BN along the (0001) basal plane of the hexagon. The factuality of the structural and stereochemical role of the h-BN phase nucleation promoter is analogous to the observation of carbon diamond by using the thermal cracking of diluted CH_4 gas which is sp^3 -hybridized as carbon in the

diamond structure. The presence of an insufficient amount of carbon causes a reduction in the number of nucleating sites for BN either in amorphous or crystalline form together with relatively higher concentration of unreduced B_2O_3 and BO gases. The presence of hydrogen with nitrogen, however, assists the gasification of carbon via hydrocarbon gas formation reaction and thereby favours the condition for BO gas generation when $\text{C}:\text{B}_2\text{O}_3$ ratio exceeds more than 3:1 in the mixtures. The gaseous carbon therefore can nucleate in a similar manner as BN and alter the crystallinity of h-BN.

With increasing temperature, the amorphous BN structure slowly relaxes to a stable crystalline structure. This is the reason that the crystallinity of high-temperature synthesized BN is much higher than the low-temperature reaction product.

4.5. General relevance of experimental findings to BN powder manufacture

The reduction-nitridation results unambiguously demonstrate that the hexagonal form of the boron nitride powder can be produced at much lower temperatures than currently adopted by large-scale powder manufacturing establishments. The formation of B_4C phase in the early stages of reaction in the core of a pellet of 8×12 mm in size is important evidence for designing an efficient powder or pellet reactor in which a uniform distribution of nitriding gas or nitriding agent can be warranted. Empirical data also suggest that the gaseous diffusion of nitrogen in the early stages of reaction is only limited to a 1–2 mm distance from the surface of the cylindrical pellet. In a packed-bed reactor, either with pellets or with powder agglomerates of uniform size, the nitrogen starvation problem could be even more serious than the single-pellet studies. This is because of a longer nitriding gas diffusion path in the reactor bed than in the single-pellet investigations.

Furthermore if the carbon is not present in sufficient quantities, a rapid loss of boron oxide either as unreacted B_2O_3 or BO gas will be expected resulting in a meagre product yield. The problem associated with the volatilization loss will become more serious if the operating reactor temperature exceeds 1773 K. On the basis of our experimental results, we propose the following features of an efficient BN reactor.

- The reactor should preferably operate in the temperature regime of 1573 to 1773 K and it must efficiently use carbothermic reduction for producing the BO gas, an essential species for sustaining the boron nitride synthesis reaction.
- The distribution of nitrogen or a nitriding gas should be uniform throughout the reactor bed, so that the reacting gas or gases can readily pore-diffuse to react with BO gas in the presence of carbon or another reducing gas for the formation of h-BN. Nitrogen gas starvation must be avoided at all cost in order to prevent the formation of B_4C phase. The formation of this phase slows the overall nitridation leading to h-BN powder production.

(c) The water of crystallization associated with boric oxide must account for the carbon balance of the reactor. The carbon balance may, as expected, vary from one reactor to another depending upon the rate of heating of the powder or pellet charge. The contribution of water to the loss of carbon as CO gas via the well-known water-shift reaction: $C(s) + H_2O(g) = CO(g) + H_2(g)$ must account for effectively sustaining the BN reaction.

5. Conclusions

The main conclusions of this investigations are as follows.

1. Hexagonal BN powder can be produced in the temperature range 1473 to 1773 K by nitriding B_2O_3 /carbon mixtures. The intermediate reaction temperature range (1573 to 1673 K) was found to be the most suitable for a complete conversion to h-BN powder.
2. The structure of the graphitic form of boron nitride strongly depends upon the structure and stereochemistry of the nucleation promoter. This is the reason that the a-BN structure grows epitaxially when boric anhydride is reduced in the presence of semicrystalline activated charcoal ($B_2O_3:C = 1:4$). Whereas even in the presence of activated charcoal, when sp^2 -hybridized ammonia gas is used as a nitriding agent, the crystalline h-BN forms.
3. The degree of crystallinity of hexagonal boron nitride after nucleation strongly depends upon the temperature. The higher temperature reaction products are more crystalline than their lower temperature structural forms.
4. In the early stages of the reduction-nitridation of B_2O_3 with carbon, B_4C forms which subsequently transforms into h-BN in the nitriding atmosphere in the presence of BO gas. The nitrida-

tion of B_4C to h-BN is favoured in the presence of hydrogen in the gas phase.

5. The nitridation of B_4C appears to yield a range of carbonitride phase having lattice parameters smaller than the carbon-saturated boron carbide.
6. The microstructural evidence strongly points out that a larger number of h-BN nuclei form in the presence of NH_3 as a nitriding gas than in the presence of nitrogen gas. This differential in the nucleation arises due to a difference in the Gibbs free energy.

Acknowledgments

The authors acknowledge financial support from the Office of Overseas Research Students, UK. AJ gratefully acknowledges support from RIST Laboratories, Pohang, South Korea for granting a leave for post graduate studies to SJY.

References

1. S. J. YOON and A. JHA, *J. Mater. Sci.* **30** (1995) 607.
2. F. THEVENOT, *J. Eur. Ceram. Soc.* **6** (1990) 205.
3. B. V. DERYAGIN and D. V. FEDOSAYEV, in "Diamond growth and films", edited by Universities' Carbon Films and Materials Group (Elsevier Applied Science Publishers Ltd, Barking, UK) p. 180.
4. A. CHRYSANTHOU, P. GRIEVESON and A. JHA, *J. Mater. Sci.* **26** (1991) 3463.
5. J. D. ESHELBY, *J. Appl. Phys.* **24** (1952) 176.
6. E. T. TURKDOGAN, "The physical chemistry of high-temperature technology" (Academic Press, London, 1980) p. 5.

*Received 30 August
and accepted 4 October 1995*